HHS Public Access

Author manuscript

Nat Commun. Author manuscript; available in PMC 2014 February 07.

Published in final edited form as:

Nat Commun. 2013 ; 4: 2285. doi:10.1038/ncomms3285.

The unusual dynamics of parasite actin result from isodesmic polymerization

Kristen M. Skillman[a,*], **Christopher I. Ma**[a,*], **Daved H. Fremont**[b], **Karthikeyan Diraviyam**[c], **John A. Cooper**[d], **David Sept**[c,1], and **L. David Sibley**[a,1]

[a]Departments of Molecular Microbiology, Washington University Sch. Med., 660 S. Euclid Ave, St. Louis MO

[b]Departments of Pathology and Immunology, Washington University Sch. Med., 660 S. Euclid Ave, St. Louis MO

[c]Department of Biomedical Engineering and Center for Computational Medicine and Bioinformatics, University of Michigan, Ann Arbor, MI 48109

[d]Departments of Cell Biology and Physiology, Washington University Sch. Med., 660 S. Euclid Ave, St. Louis MO

Abstract

Previous reports have indicated that parasite actins are short and inherently unstable, despite being required for motility. Here, we re-examine the polymerization properties of actin in *Toxoplasma gondii* (TgACTI), unexpectedly finding that it exhibits isodesmic polymerization in contrast to the conventional nucleation-elongation process of all previously studied actins from both eukaryotes and bacteria. TgACTI polymerization kinetics lacks both a lag phase and critical concentration, normally characteristic of actins. Unique among actins, the kinetics of assembly can be fit with a single set of rate constants for all subunit interactions, without need for separate nucleation and elongation rates. This isodesmic model accurately predicts the assembly, disassembly, and the size distribution of TgACTI filaments *in vitro*, providing a mechanistic explanation for actin dynamics *in vivo*. Our findings expand the repertoire of mechanisms by which actin polymerization is governed and offer clues about the evolution of self-assembling, stabilized protein polymers.

Actin shares a common fold with a superfamily of proteins that includes sugar kinases, Hsp70, and actin-related proteins, including bacterial homologues of actin (*i.e*. MreB, ParM, etc.,)[1]. Among this group, actins characteristically cycle between monomeric and filamentous forms using a nucleation-elongation mechanism for polymerization, which

[1]To whom correspondence should be addressed. Sibley@borcim.wustl.edu.
[*]Contributed equally to the experimental studies
Contributed equally as senior, co-corresponding authors: DS (dsept@umich.edu) and LDS (Sibley@borcim.wustl.edu).

Author contribution

Conceived and designed the experiments: KMS, CIM, DHF, KD, JAC, DS, LDS; Performed the wet lab experiments KMS, CIM; Performed the simulations, molecular dynamics and modeling: KD, DS; Analyzed the data: KMS, CIM, DHF, KD, JAC, DS, LDS; Wrote the paper: KMS, JAC, DS, LDS.

Competing financial interests: The authors declare no competing financial interests.

supports structure, mechanics, and motility in cells[2]. Apicomplexan parasites, such as *Toxoplasma* and *Plasmodium*, are ancient, divergent eukaryotes that also require on actin polymerization for motility[3,4] and active invasion of host cells[5]. Despite this requirement, the vast majority of parasite actin remains unpolymerized *in vivo*[6,7] and purified parasite actins form very short filaments *in vitro*[8,9,10]. Actin in *T. gondii*, TgACTI, is only ~80% identical to mammalian or yeast actin[6] and differences in the molecular interactions responsible for inter-strand filament contacts contribute to the instability of parasite actins[11]. It has remained enigmatic how the seemingly inefficient polymerization and transient nature of actin filaments support motility in these organisms.

Conventional actins, as well as the actin-related protein Arp1, undergo cooperative assembly to polymerize head-to-tail into two inter-twined helical strands that form a filament[12]. Polymerization occurs by a nucleation-elongation mechanism, in which filaments elongate rapidly from nuclei that assemble slowly and only if the actin concentration exceeds a characteristic critical concentration (Cc)[13]. Polymerization from monomeric subunits displays a slow nucleation step due to the instability of dimer and trimer intermediates, resulting in a lag phase in the time course of polymerization[14]. In contrast to a nucleation-elongation mechanism, protein polymers can theoretically assemble by an isodesmic mechanism, which is non-cooperative and does not require a nucleus to initiate polymerization[15,16]. During isodesmic polymerization, all monomer-polymer interactions occur with equal affinity and the amounts of both monomer and polymer increase with total protein concentration, in contrast to cooperative assembly, where the monomer concentration plateaus upon reaching the Cc[15]. All well-studied actins, from yeast, amoeba, and animal cells[12], as well as bacterial actin-like homologues[17], display nucleation-elongation polymerization, which is generally regarded as a conserved property of actins.

Given the unusual nature of parasite actins, we challenged the assumption that a standard nucleation-elongation mechanism could account for actin polymerization in more distant eukaryotic species such as *T. gondii*. Our findings indicate that TgACTI actin assembles by a process that is largely isodesmic, thus revealing a novel means of assembly for a cytoskeletal protein polymer. These findings have implications for the regulation of assembly and turnover of filaments that help explain the unusual actin dynamics observed *in vivo*.

Results

TgACTI exhibits unusual polymerization kinetics

We began by re-examining the polymerization of TgACTI by light scattering, using recombinant protein purified from baculovirus as described previously[11]. Polymerization was very limited at low protein concentrations but increased steadily over time at higher concentrations (Fig. 1A). Notably, the time course displayed no lag in the initiation of TgACTI polymerization at any of the concentrations tested (Fig. 1A). A previous study of the polymerization kinetics of TgACTI, as determined by tryptophan quenching, reported a lag phase, but only at very low concentrations of protein[8]. Indeed, a lag phase is not exclusive to a nucleation-elongation mechanism, since this feature can also be observed for an isodesmic process when $k_{off} > k_{on}$[18]. When we examined the initial time of

polymerization by light scattering over a wide range of concentrations, no lag phase was present (Fig. 1A, right). Instead, the rate of polymerization increased in proportional to the concentration of protein, and continued to rise over the 2 h time frame (Fig. 1A). In contrast, actin from the yeast *Saccharomyces cerevisiae* (ScACT), expressed in baculovirus and purified in parallel, showed the typical lag, elongation, and plateau phases characteristic of conventional actins (Fig. 1B)[13,14].

The differences between yeast and TgACTI polymerization were apparent despite the fact that light scattering is not directly proportional to filament mass because the light scattering signal is also influenced by bundling. With some other methods, such as fluorescence of pyrene-actin, the signal is proportional only to filament mass[19]. In the pyrene-actin method, actin is labeled with pyrene on a conserved cysteine residue. TgACTI has this conserved cysteine (Cys375), and we were able to label Cys375 with pyrene. However, we found that pyrene- TgACTI did not show enhanced fluorescence when polymerization was induced (C. Ma unpublished). Although the effects of bundling on the signal meant that we were not able to directly model the assembly kinetics from the light scattering traces, dramatic differences were evident between the traditional nucleation-elongation process exhibited by yeast actin and the unconventional process exhibited by TgACTI.

Although TgACTI showed evidence of polymerization by light scattering, it did not form conventional length filaments detectable by fluorescence phalloidin staining unless incubated with equimolar concentrations of phalloidin (i.e. at 5 μM) (Fig. 1C), consistent with previous reports[11]. This requirement was overcome at higher protein concentrations (i.e. 25–40 μM), allowing visualization of bundles of long filaments that were detected by adding trace amounts of labeled phalloidin and fluorescence microscopy (Fig. 1C). When a high concentration of TgACTI was polymerized in F buffer and examined by quick-freeze, deep-etch electron microscopy, occasional filament bundles were surrounded by many small heterogeneously sized oligomers and short filaments ranging from 25–100 nm, which are similar to previous *in vivo* measurements[8] (Fig. 1D, E). In contrast, ScACT formed much longer filaments (i.e. 500–1,500 nm) with a typical right-handed helical pattern of two protofilaments, which also occasionally formed bundles (Fig. 1D, E). The short filaments formed by TgACTI had a conventional double-stranded structure but showed less evidence of a helical pattern when compared to ScACT (Fig. 1D). The failure of TgACTI to form filaments at lower concentrations was not due to a general defect in folding because circular dichroism measurements indicated a similar secondary structure to that of yeast actin (Fig. 1F).

Inefficient sedimentation of heterogeneous TgACTI filaments

When conventional actins undergo polymerization, nearly all of the polymer assumes the form of long filaments that sediment efficiently at 100,000*g*[20]. Previous studies using low concentrations (i.e. below 5 μM) of TgACTI have reported that sedimentation requires higher *g* forces than conventional actins (i.e. 350,000*g* for 1 h)[8]. Given our findings for concentration dependence of TgACTI polymerization above, we examined the influence of protein concentration on the efficiency of sedimentation. When 5 μM TgACTI was polymerized in F buffer and centrifuged at 100,000*g*, ~30% of the protein appeared in the

pellet (Fig. 2A, top). Addition of phalloidin at an equimolar ratio caused a greater fraction of TgACTI to shift to the pellet (~60%) (Fig. 2A, top). In contrast, centrifugation at 350,000*g* was sufficient to pellet the majority of TgACTI, both in the presence and absence of phalloidin (~85–90%) (Fig. 2A, top). At higher protein concentration (i.e. 30 μM), ~37% of TgACTI pelleted on centrifugation at 100,000*g* (Fig. 2A, middle). Addition of phalloidin and centrifugation at 100,000*g*, or centrifugation at 350,000*g*, was sufficient to sediment nearly all of the TgACTI (~90%) (Fig. 2A, middle). In comparison, more than 90% of ScACT, expressed and purified in the same manner as TgACTI, was found in the pellet after incubation in F buffer regardless of the centrifugation speed or the presence of phalloidin (Fig. 2A, bottom). These findings indicate that although TgACTI undergoes dose-dependent polymerization, it forms oligomers that sediment far less efficiently than conventional actins.

To evaluate the size distribution of polymerized TgACTI, samples were subjected to density gradient centrifugation. When 5 μM TgACTI incubated in non-polymerizing G buffer was analyzed by sucrose gradient sedimentation, the majority of protein was found near the top of the gradient (Fig. 2B, top). At higher protein concentrations (i.e. 30 μM) in G buffer, TgACTI sedimented more rapidly, appearing farther down the gradient (Fig. 2B, middle). Incubation of 5 μM or 30 μM TgACTI in polymerizing F buffer shifted the protein distribution further down the gradient, although the majority of protein was still found in lighter fractions under both conditions (Fig. 2B). Following addition of phalloidin, ~15% of the 5 μM actin was shifted to the pellet, while the majority of 30 μM actin sedimented into the pellet (Fig. 2B). In contrast to the heterogeneous behavior of TgACTI, sucrose gradient sedimentation of ScACT produced two discrete populations at opposite ends of the gradient. In G buffer, the majority of ScACT was found in light fractions (S < 4.4 standard for BSA), likely corresponding to monomers and a mixture of dimers (Fig. 2B, bottom). However, in F buffer, the majority of ScACT was found in the pellet, consistent with polymerization into long filaments (Fig. 2B, bottom). In order to estimate the size of TgACTI polymers, we estimated the proportion of actin found in the pellet after F buffer incubation and high-speed centrifugation at 100,000*g* or 350,000*g* (data from 2A). These estimated amounts of pelleted actin were plotted against the cumulative fractions of the sucrose gradients (Fig. 2B, dashed line, solid line, respectively), in order to estimate the relative size of the filaments. From this comparison, it was evident that TgACTI filaments are not long, like those of yeast, which sediment rapidly. In contrast, TgACTI filaments are much shorter, and their length distribution is more heterogeneous.

To provide a better estimate of the sizes of actin oligomers formed by TgACTI, we examined protein samples by dynamic light scattering and used an autocorrelation function to estimate hydrodynamic radius (Rh), mass, and polydispersity. Yeast actin (ScACT) suspended in G buffer was detected primarily as a single peak with a hydrodynamic radius of 3.6 nm and approximate mass of 67 kDa (Table 1). This size estimate likely represents an average of monomer (estimated Rh 3.0)[21] and dimer forms (estimated Rh 3.8–4.1 for low-pitch and high-pitch dimer, respectively, as estimated using Stokes-Einstein theory). Addition of F buffer to ScACT shifted the size to the upper end of the spectrum that was detectable by the instrument (i.e. $>10^9$ kDa), consistent with assembly of actin into long

polymers (Table 1). The behavior of TgACTI in G buffer indicated a much larger average hydrodynamic radius and mass than predicted for monomer, consistent with a range of small oligomers from 2–5 subunits at 1 μM that shifted to 5–10 subunits at 5 μM (Table 1, Supplementary Table S1). Addition of F buffer shifted the size of TgACTI to an intermediate range with an average size of ~7,000 kDa, and a much broader polydispersity, consistent with a variety of oligomers from 35~500 subunits, but without the extremely large polymers seen in ScACT (Table 1, Supplementary Table S1). The estimated size of TgACTI oligomers formed in G buffer is consistent with globular aggregates previously reported by EM[8,11], and the size distribution in F buffer corresponds to observations of filaments observed by EM above, and reported previously[8,11]. The length distribution of TgACTI filaments depended on the concentration of TgACTI in a continuous manner, with longer filaments at higher concentrations of protein. In contrast, the length distribution of ScACT filaments displayed an abrupt transition to a population of long filaments when the protein concentration exceeded the critical concentration (Cc) (Fig. 1D, Table 1, Supplementary Table S1). These different behaviors of filament length with respect to protein concentration are consistent with predictions based on isodesmic vs. nucleation-elongation modes of assembly.

TgACT1 polymerizes by an isodesmic process

Having established that TgACTI polymerizes more robustly at higher concentrations than were used in previous analyses, we revisited the question of the existence of a critical concentration. We examined the amount of protein in the supernatant and pellet after incubation for 1 h at room temperature in F buffer pH 8.0 and centrifugation for 1 h at 100,000*g*. If TgACTI underwent nucleation-elongation polymerization similar to conventional actins, the concentration of protein in the supernatant would be expected to plateau at the Cc[13,14]. Strikingly, this was not observed. Rather, the amount of protein in the supernatant continued to increase up to 100 μM TgACTI, the highest concentration tested (Fig. 3A). The absence of a clear plateau in the supernatant was also observed when TgACTI was polymerized in KMEI pH 7.2 (Fig. 3B), indicating this behavior is not due to some unusual salt or pH preference. In contrast, polymerization of yeast actin (ScACT) under similar conditions showed a marked plateau in the concentration of the supernatant, and a clear Cc below which polymer was not detected (Fig. 3C). Purified TgACTI was also polymerized for 20 h, and the steady-state levels of polymerization were measured by light scattering, as described previously[11]. The amount of polymerized TgACTI increased proportionally to the total amount used in the reaction, and this data was fit using a linear or quadratic equation (Fig. 3D). The intercept of this curve crosses the x-axis at very low concentration, but there was no range where polymerization did not occur (Fig. 3D inset). When TgACTI polymerization reactions were allowed to go to steady state (i.e. > 20 h) and separated by sedimentation, again there was no obvious Cc, although above 10 μM, the majority of TgACTI was found in the pellet (Fig. 3E). Collectively, these results are inconsistent with a fixed critical concentration typical of a nucleation-elongation mechanism, but instead are explained by an isodesmic mechanism of polymerization.

We modeled the polymerization kinetics of TgACTI based on sedimentation assays using either conventional nucleation-elongation mechanism, as described previously[22], or an

isodesmic interaction, where the association and dissociation rate constants were assumed to be the same for each step in the polymerization reaction (Fig. 4A). Surprisingly, the isodesmic model does an excellent job of describing the extent of polymerization over the full range of actin concentrations (Fig. 4B). The isodesmic model predicts rate constants of k_{on}= 5.9×10^{-5} μM^{-1} s^{-1} and k_{off}= 4.0×10^{-4} s^{-1}, both remarkably low in comparison to the rate constants for elongation of conventional actin, for which the on-rate constant is typically ~10 μM^{-1} s^{-1}[12,22]. The rate constants for TgACTI give a binding affinity of 6.8 μM, consistent with the observed low rate of TgACTI polymerization at low concentrations and increased abundance of filaments with increasing concentration. Simulation of the polymerization kinetics using the isodesmic model generated curves that closely matched the proportion of TgACTI in the supernatant vs. pellet at both 1 h and 20 h (curves in Fig. 3A,D). Structural modeling and molecular dynamics supports a role for an isodesmic mechanism in explaining the behavior of TgACTI. Molecular dynamics simulation of muscle *vs*. TgACTI filaments confirms that much weaker lateral interactions are formed between protofilaments (Fig. 4D), consistent with previously identified residues that affect lateral contacts and filament stability[11] (Fig 4C).

Although this simple isodesmic model predicts the polymerization behavior of TgACTI, across a range of concentrations, it does not address the depolymerization behavior of filaments once they form. To examine this directly, we polymerized TgACTI at 20 μM in F buffer overnight, then diluted it by 4-fold, a concentration below the threshold where most of the actins form polymers of sufficient mass to sediment at 100,000*g* (Fig 3A). We observed a very gradual but significant decline in light scattering after dilution, which supports the conclusion that polymers of TgACTI have a slow off rate. Again the isodesmic model accurately fits the observations (Fig. 3F), but since there is no critical concentration, dilution results in loss of >30 % of the polymer. In contrast, when ScACT filaments were diluted under similar conditions, they underwent more modest depolymerization and reached a new steady state where the free monomer concentration again equaled the critical concentration (Cc, Fig. 3F). ScACT depolymerization was accurately described by a nucleation-elongation model (Fig 3F), which predicts only minor loss of polymer (i.e ~ 5%). Collectively, these observations fit the expectation that conventional actins are robust to depolymerization because they are naturally buffered by their Cc, while TgACTI respond more dramatically to alterations in concentration, thus resulting in filaments that are less stable.

Discussion

Collectively, our findings reveal that TgACTI slowly polymerizes to form a heterogeneous mixture of relatively short filaments, resulting in a length distribution remarkably different from that of conventional actins. This discovery explains previous differences from conventional actins and offers insight into the behavior of parasite actin *in vivo*. First, nucleation is not rate limiting, so that *T. gondii* does not need nucleation-promoting factors. Indeed, homologs of actin nucleating proteins, such as Arp2/3 complex, have not been identified within apicomplexan genomes[23]. Second, an isodesmic mechanism results in a distribution of small oligomers, which explains why TgACTI only sediments efficiently at higher *g* force[6,24]. Our findings also explain why long TgACTI filaments have not been

observed in parasites by any method, including electron microscopy, fluorescence imaging of GFP-TgACTI, and phalloidin staining[6,8,11,24]. Other parasite actin binding proteins are also adapted to this difference in kinetics, for example ADF acts primarily as a sequestering agent while exhibiting minimal severing activity[25], which is consistent with an absence of stable filaments. As predicted by an isodesmic model, EM showed a distribution of heterogeneously sized small oligomers and short filaments ranging in size from 25 nm-100 nm in length (Fig. 1E, excluding bundles which may form by annealing of individual filaments). This size distribution is similar to filaments that form *in vivo* during gliding motility (Fig. 1E and[8]).

Previous studies have also shown that *T. gondii* has a streamlined repertoire of actin binding proteins including actin depolymerizing factor (ADF) and profilin[25,26]. The ADF of *T. gondii* is somewhat unusual in functioning largely in sequestration of G-actin; the concentration of G-actin is ~ 35 μM in the cytosol while that of TgACTI is ~ 40 μM[25]. Combined with the affinity of TgADF1 for TgACTI (i.e. 0.8 μM) it is likely that the majority of TgADF1 is bound to TgACTI[25]. In this regard, profilin has also been shown to function in sequestering TgACTI (~ 38 μM cytosolic concentration and a dissociation binding constant of ~5 μM)[26]. Collectively, ADF and profilin should then combine to keep the concentration of free TgACTI monomer very low (i.e. below 5 μM), a level that would only allow for the filaments to be short and of variable length. The robust control of free TgACTI levels, and hence the distribution of filament lengths, would appear to be of critical importance, based on the observation that disruption of the genes encoding TgADF[27] or profilin[28] leads to profound defects in cell motility and cell invasion. Hence, isodesmic polymerization is better suited than nucleation-condensation for the assembly of short filaments and oligomers, which function in parasite motility, rather than the long, stable filaments that represent the functioning form of F-actin in yeast and mammalian cells.

Importantly, the fact that TgACTI undergoes isodesmic assembly does not make any a priori predictions about the directionality of assembly or the structure of the filament. Directionality during filament growth is determined by the on- and off-rate constants at the two ends of the filament, which are not required to be the same in an isodesmic process. Likewise the net rate of assembly/disassembly may differ at the two ends, although such as difference would require energy, likely provided by ATP hydrolysis as is true for actins in general[29]. Determining the directionality of assembly is an important future goal that awaits methods for single molecule imaging of TgACTI polymerization.

An isodesmic polymerization process also does not imply that the structure of the TgACTI filament include only a single protofilament. The reactions from monomer to dimer, dimer to trimer, and so forth, must have similar binding constants. The structural basis of this biochemical process is an open question that will require atomic-level structural and mutational analysis for proper resolution. At this point, we know that TgACTI filaments viewed by electron microscopy appear to display two protofilaments; however, the resolution was not sufficient to reveal whether the protofilaments are in a helical conformation. The filament may be in a relaxed conformation due to an intrinsically lower contribution of intrastrand interactions to filament stability, consistent with previous reports showing that TgACTI contains natural substitutions in residues that normally stabilize

lateral interactions between the two protofilaments[11]. Thus, the subunit interactions that dominate during filament assembly may be arranged in a one-start helix. Bacterial actin-like proteins also form a variety of filament types ranging from single strand protofilaments (i.e. MreB) to both right and left-handed helices comprised of two protofilaments[17]. Collectively, these findings indicate that actin can adopt a wider range of conformations and assembly processes than reflected by conventional actins in animal cells.

Actin and related proteins have evolved to form higher order assemblies that perform mechanical work and impart structural rigidity[12]. Conventional eukaryotic actins use cooperative assembly to generate filaments with strong inter-strand contacts[30]. Prokaryotic actins such as the bacterial actin homolog MreB form both single-stranded helices and linear double-stranded filaments[31,32], yet polymerization occurs by a nucleation-elongation mechanism with a critical concentration of ~ 0.9 μM[33]. In contrast, TgACTI represents a different evolutionary strategy, utilizing an isodesmic process to form a double-stranded filament that lacks a cooperative mechanism of assembly and features weak inter-strand filament interactions. Our findings predict that other unconventional actins may also undergo a similar process of isodesmic polymerization. For example, *Plasmodium* ACTI shares many of the properties of TgACTI[11], as do actins in many plants[34,35] and protozoan parasites[36,37,38]. In all these cases, actins exhibit unusual polymerization kinetics and remain primarily unpolymerized *in vivo*. Collectively these observations are consistent with actin having adapted different modes of polymerization to support a diverse array of structural and motile processes in cells.

Methods

Actin expression and purification

TgACTI or ScACT were expressed and purified from baculovirus as described previously[11]. In brief, His-tagged actins were purified using Ni-NTA agarose (Invitrogen) and stored in G actin buffer (5 mM Tris-Cl, pH 8.0, 0.2 mM $CaCl_2$, 0.2 mM ATP) containing 0.5 mM DTT with 100 μM sucrose. Purified actins were quantified as described[11], stored at 4°C, and used within 2–3 d. Prior to use, purified actins were clarified by centrifugation at 100,000*g*, 4°C, for 30 min using a TL100 rotor and a Beckman Optima TL ultracentrifuge (Beckman Coulter, Brea, CA). Polymerization properties of actins diluted in G-buffer were examined following addition F- buffer (final: 50 mM KCl, 2 mM $MgCl_2$, 1 mM ATP, 1 mM EGTA at pH 8.0) or in KMEI (final: 50 mM KCl, 10 mM imidazole, 2 mM $MgCl_2$, 1 mM EGTA, pH 7.2).

Light Scattering

Actins were diluted in G buffer, and polymerization was induced by addition of F buffer pH 8.0 (with 1 mM EGTA to replace bound Ca^{2+} with Mg^{2}). Polymerization was induced by addition of F buffer pH 8.0. Ninety-degree light scattering was monitored in a 100 μl cuvette (Submicro Quartz Fluorometer cell, Starna Cells, Atascadero, CA) using a PTI Quantmaster spectrofluorometer (Photon Technology International, Santa Clara, CA): excitation 310 nm (1 nm bandpass), emission 310 nm (1 nm bandpass), as described previously[11]. Data were collected either during the first 100 min to capture initial kinetics, or after 20 h to establish

the steady state level of polymerization (as established by testing different time intervals). The average reading at 20 h was plotted *vs*. protein concentration and analyzed using linear and nonlinear functions (Prism, GraphPad). To properly normalize the depolymerization data, we rescaled the data based on knowledge of the expected starting and ending F-actin concentrations based on sedimentation experiments.

Polymerization Model

To describe the polymerization kinetics we adopted an isodesmic polymerization model. This model assumes that the association and dissociation rate constants are identical for all steps of the polymerization reaction. We explicitly modeled each polymer length by solving the coupled set of differential equations for the set of reactions

$$\frac{dA_1}{dt} = -k_{\text{on}}A_1(2A_1 + \sum_{i\geq 2} A_i) + k_{\text{off}}(2A_2 + \sum_{i\geq 3} A_i) \quad (1)$$

$$\frac{dA_i}{dt} = -k_{\text{on}}A_1A_i + k_{\text{off}}A_{i+1} \text{for} i \geq 2 \quad (2)$$

keeping track of all polymers up to a length of i=100 protomers. The amount of polymer was simply taken as the sum of all oligomers (dimers, trimers, etc.) and this quantity was used for comparison with both the light scatting and sedimentation data. The set of rate constants that gave us the best least-squares fits to the polymerization and depolymerization data were k_{on}= 5.9×10^{-5} μM^{-1} s^{-1} and k_{off} = 4.0×10^{-4} s^{-1}

Molecular dynamics simulations

We used the results of molecular dynamics simulations described previously[11]. The pairwise contact surface area was calculated and averaged over all protomers using VMD[39].

Fluorescence Microscopy

Purified recombinant actins were diluted in F buffer pH. 8.0 ± equimolar unlabeled phalloidin (Molecular Probes, Eugene, OR) and Alexa-488 phalloidin (0.33 μM) (Molecular Probes), incubated for 1 h and viewed with a Zeiss Axioskop (Carl Zeiss, Thornwood, NY) using 63× Plan-NeoFluar oil immersion lens (1.30 NA). Images were collected using a Zeiss Axiocam with Axiovision v3.1 and processed by linear adjustment using Photoshop v8.0 (Adobe, San Jose, CA).

Electron Microscopy

Purified recombinant TgACTI and ScACT were diluted to 40 μM and 5 μM, respectively in F buffer and polymerized for 1 h. Quick-freeze, deep-etch electron microscopy (EM) of samples on mica was performed as described previously[40]. Replicas were mounted on formvar-coated copper grids, and photographed with a JEOL 1400 microscope (Tokyo, Japan) with AMT digital camera (Woburn, MA).

Actin Sedimentation Assays

Purified recombinant actins were diluted in G- buffer and then incubated in F buffer pH 8.0 or KMEI (pH 7.2) for 1 h at room temperature and centrifuged at 100,000*g* using a TL100 rotor and Beckman Optima TL ultracentrifuge. To examine the effects of phalloidin on polymerization, samples were incubated in F buffer pH 8.0 ± equimolar unlabeled phalloidin (Molecular Probes) for 1 h at room temperature and centrifuged at 100,000*g* or 350,000*g* for 1 h at room temperature. Acetone-precipitated supernatants and pellets were resolved on a 12% SDS-PAGE gels, stained with Sypro-Ruby (Molecular Probes), visualized using a FLA-5000 phosphorimager (Fuji Film Medical Systems), and quantified using Image Gauge v4.23. To establish the extent of polymerization at steady state, samples were polymerized in F buffer pH 8.0 for 20 h at room temperature and sedimented at 100,000*g*. The ratio of the pellet / total actin at 20 h was plotted using a sigmoidal dose response (Prism, GraphPad).

Density Centrifugation

Purified recombinant actins were incubated with 1 mM EGTA and 50 μM $MgCl_2$ for 10 min (to replace bound Ca^{2+} with Mg^{2+}). Actins were incubated in G buffer, F buffer pH 8.0 or F buffer supplemented with equimolar phalloidin (Molecular Probes) for 1 h at room temperature. Samples were loaded on the top of 11 ml 5–40% continuous sucrose gradients, made in the corresponding buffer using a Auto Densi-Flow Gradient Fractionator (LabConco, Kansas City, MO), and centrifuged at 100,000g, 4°C for 20 h using a SW41 rotor in a L-80 ultracentrifuge (Beckman Coulter). Bovine serum albumin, 4.4S, lactate dehydrogenase, 7S, catalase, 11.4S, thyroglobulin, 19.4S (HMW Calibration kit, GE Healthcare, Buckinghamshire, UK) were used for density standards. The specific gravity of each fraction was measured using a refractometer (Sper Scientific, Scottsdale, AZ). Fractions were precipitated in 10% TCA for 1 h, resolved on 12% SDS-PAGE gels, stained with Sypro-Ruby (Molecular Probes), visualized using a FLA-5000 phosphorimager (Fuji Film Medical Systems) and Image Gauge v4.23.

Dynamic Light Scattering

Purified recombinant TgACTI and ScACT were clarified as described above and diluted to either 1 μM or 5 μM in G buffer or to 1 μM or 5 μM in F buffer pH 8.0 and polymerized for 1 h. Dynamic light scattering was performed using DynaPro- MSXTC (Wyatt Technology, Santa Barbara, CA) and analyzed using Dynamics V6.3.4.0 software (Wyatt Technology).

Circular dichroism

Purified recombinant actins were diluted to 0.4 μM in 0.8 M sodium fluoride buffer and loaded into a 10 mm cuvette for measurement. CD spectra were monitored at 200 to 250 nm using a Jasco J-810 Spectrometer (Jasco Analytical Instruments, Easton, MD). Data were plotted using Prism (GraphPad).

Estimation of hydrodynamic radii

To estimate the hydrodynamic radii of different sized actin oligomers, we used the Oda *et al*., actin filament structure[30] and created structures for the monomer, low-pitch and high-pitch dimers, trimers, etc. Using HYDROPRO[41] we calculated the translational diffusion

contact at 20° C and used this value to determine the corresponding hydrodynamic radius, based on Stokes-Einstein theory.

Supplementary Material

Refer to Web version on PubMed Central for supplementary material.

Acknowledgements

We thank Melissa Barrow for advice on dynamic light scattering, Tom Brett for advice on circular dichroism, and Carl Frieden and John Heuser for helpful discussions. Electron microscopy was performed by Robyn Roth, Laboratory of Electron Microscopy Sciences, Department of Cell Biology, Washington University School of Medicine. Supported by predoctoral fellowships from the American Heart Association (0815645G to K.M.S.) and grants from the NIH (AI073155 to L.D.S, D.S and GM38542 to J.A.C.).

References

1. Kabsch W, Holmes KC. The actin fold. FASEB J. 1995; 9:167–174. [PubMed: 7781919]
2. Pollard TD, Cooper JA. Actin, a central player in cell shape and movement. Science. 2009; 326:1208–1212. [PubMed: 19965462]
3. Håkansson S, Morisaki H, Heuser JE, Sibley LD. Time-lapse video microscopy of gliding motility in *Toxoplasma gondii* reveals a novel, biphasic mechanism of cell locomotion. Mol. Biol. Cell. 1999; 10:3539–3547. [PubMed: 10564254]
4. Munter S, et al. Plasmodium sporozoite motility is modulated by the turnover of discrete adhesion sites. Cell Host Microbe. 2009; 6:551–562. [PubMed: 20006843]
5. Dobrowolski JM, Sibley LD. Toxoplasma invasion of mammalian cells is powered by the actin cytoskeleton of the parasite. Cell. 1996; 84:933–939. [PubMed: 8601316]
6. Dobrowolski JM, Niesman IR, Sibley LD. Actin in the parasite *Toxoplasma gondii* is encoded by a single copy gene *ACT1* and exists primarily in a globular form. Cell Motil. Cytoskel. 1997; 37:253–262.
7. Schmitz S, et al. Malaria parasite actin filaments are very short. J. Mol. Biol. 2005; 349:113–125. [PubMed: 15876372]
8. Sahoo N, Beatty WL, Heuser JE, Sept D, Sibley LD. Unusual kinetic and structural properties control rapid assembly and turnover of actin in the parasite *Toxoplasma gondii*. Mol. Biol. Cell. 2006; 17:895–906. [PubMed: 16319175]
9. Schmitz S, et al. Malaria parasite actin polymerisation and filament structure. J Biol Chem. 2010; 285:36577–36585. [PubMed: 20826799]
10. Schüler H, Mueller AK, Matuschewski K. Unusual properties of *Plasmodium falciparum* actin: new insights into microfilament dynamics of apicomplexan parasites. FEBS Letters. 2005; 579:655–660. [PubMed: 15670824]
11. Skillman KM, et al. Evolutionarily divergent, unstable filamentous actin is essential for gliding motility of apicomplexan parasites. PLoS Pathogens. 2011; 7:e1002280. [PubMed: 21998582]
12. Pollard TD, Blanchoin L, Mullins RD. Molecular mechanisms controlling actin filament dynamics in nonmuscle cells. Annu. Rev. Biophys. Biomol. Struct. 2000; 29:545–576. [PubMed: 10940259]
13. Nishida E, Sakai H. Kinetic analysis of actin polymerization. J. Biochem. 1983; 93:1011–1020. [PubMed: 6863231]
14. Cooper JA, Buhle EL, Walker SB, Tsong TY, Pollard TD. Kinetic evidence for a monomer activation step in actin polymerization. Biochemistry. 1983; 22:2193–2202. [PubMed: 6860660]
15. Miraldi ER, Thomas PJ, Romberg L. Allosteric models for cooperative polymerization of linear polymers. Biophys J. 2008; 95:2470–2486. [PubMed: 18502809]
16. Oosawa F, Kasai M. A theory of linear and helical aggregations of macromolecules. J Mol Biol. 1962; 4:10–21. [PubMed: 14482095]
17. Popp D, Robinson RC. Many ways to build an actin filament. Molec. Micro. 2011; 80:300–308.

18. Frieden C. Protein aggregation processes: In search of the mechanism. Protein Sci. 2007; 16:2334–2344. [PubMed: 17962399]
19. Cooper JA, Walker SB, Pollard TD. Pyrene actin: documentation of the validity of a sensitive assay for actin polymerization. J Muscle Res Cell Motil. 1983; 4:253–262. [PubMed: 6863518]
20. Pardee JD, Spudich JA. Purification of muscle actin. Methods Cell Biol. 1982; 24:271–289. [PubMed: 7098993]
21. Kanzaki N, Uyeda TQ, Onuma K. Intermolecular interaction of actin revealed by a dynamic light scattering technique. J Phys Chem B. 2006; 110:2881–2887. [PubMed: 16471898]
22. Sept D, McCammon JA. Thermodynamics and kinetics of actin filament nucleation. Biophys. J. 2001; 81:667–674. [PubMed: 11463615]
23. Gordon JL, Sibley LD. Comparative genome analysis reveals a conserved family of actin-like proteins in apicomplexan parasites. BMC Genomics. 2005; 6:e179.
24. Wetzel DM, Hakansson S, Hu K, Roos D, Sibley LD. Actin filament polymerization regulates gliding motility by apicomplexan parasites. Mol Biol Cell. 2003; 14:396–406. [PubMed: 12589042]
25. Mehta S, Sibley LD. *Toxoplasma gondii* actin depolymerizing factor acts primarily to sequester G-actin. J. Biol. Chem. 2010; 285:6835–6847. [PubMed: 20042603]
26. Skillman KM, Daher W, Ma CI, Soldati-Favre D, Sibley LD. *Toxoplasma gondii* profilin acts primarily to sequester G-actin while formins initiate actin filament formation in vitro. Biochem. 2012; 51:2486–2495. [PubMed: 22397711]
27. Mehta S, Sibley LD. Actin depolymerizing factor controls actin turnover and gliding motility in *Toxoplasma gondii*. Molec. Biol. Cell. 2011; 22:1290–1299. [PubMed: 21346192]
28. Plattner F, et al. *Toxoplasma* profilin is essential for host cell invasion and TLR11-dependent induction of an interleukin-12 response. Cell Host Microbe. 2008; 3:77–87. [PubMed: 18312842]
29. Pollard TD, Borisy GG. Cellular motility driven by assembly and disassembly of actin filaments. Cell. 2003; 112:453–465. [PubMed: 12600310]
30. Oda T, Iwasa M, Aihara T, Maeda Y, Narita A. The nature of the globular- to fibrous-actin transition. Nature. 2009; 457:441–445. [PubMed: 19158791]
31. Popp D, et al. Filament structure, organization, and dynamics in MreB sheets. J Biol Chem. 2010; 285:15858–15865. [PubMed: 20223832]
32. van den Ent F, Amos LA, Lowe J. Prokaryotic origin of the actin cytoskeleton. Nature. 2001; 413:39–44. [PubMed: 11544518]
33. Mayer JA, Amann KJ. Assembly properties of the Bacillus subtilis actin, MreB. Cell Motil Cytoskeleton. 2009; 66:109–118. [PubMed: 19117023]
34. Gibbon BC, Kovar DR, Staiger CJ. Latrunculin B has different effects on pollen germination and tube growth. Plant Cell. 1999; 11:2349–2363. [PubMed: 10590163]
35. Snowman BN, Kovar DR, Shevchenko G, Franklin-Tong VE, Staiger CJ. Signal-mediated depolymerization of actin in pollen during the self-incompatibility response. Plant Cell. 2002; 14:2613–2626. [PubMed: 12368508]
36. DeMelo LD, et al. Evolutionary conservation of actin-binding proteins in Trypanosoma cruzi and unusual subcellular localization of the actin homologue. Parasitology. 2008; 135:955–965. [PubMed: 18477418]
37. Paredez AR, et al. An actin cytoskeleton with evolutionaryly conserved functions in the absence of cannonical actin-binding protiens. PNAS. 2011; 108:6151–6156. [PubMed: 21444821]
38. Sahasrabuddhe AA, Bajpai VK, Gupta CM. A novel form of actin in Leishmania: molecular characterisation, subcellular localisation and association with subpellicular microtubules. Mol Biochem Parasitol. 2004; 134:105–114. [PubMed: 14747148]
39. Humphrey W, Dalke A, Schulten K. VMD: visual modeling dynamics. Graph. 1996; 14:33–38.
40. Heuser JE. Procedure for freeze-drying molecules adsorbed to mica flakes. J Mol Biol. 1983; 169:155–195. [PubMed: 6684695]
41. Ortega A, Amoroa D, GarciadelaTorre J. Prediction of hydrodynamic and other solution properties of rigid proteins from atomic and residue-level models. Biophysical. J. 2011; 101:892–898.

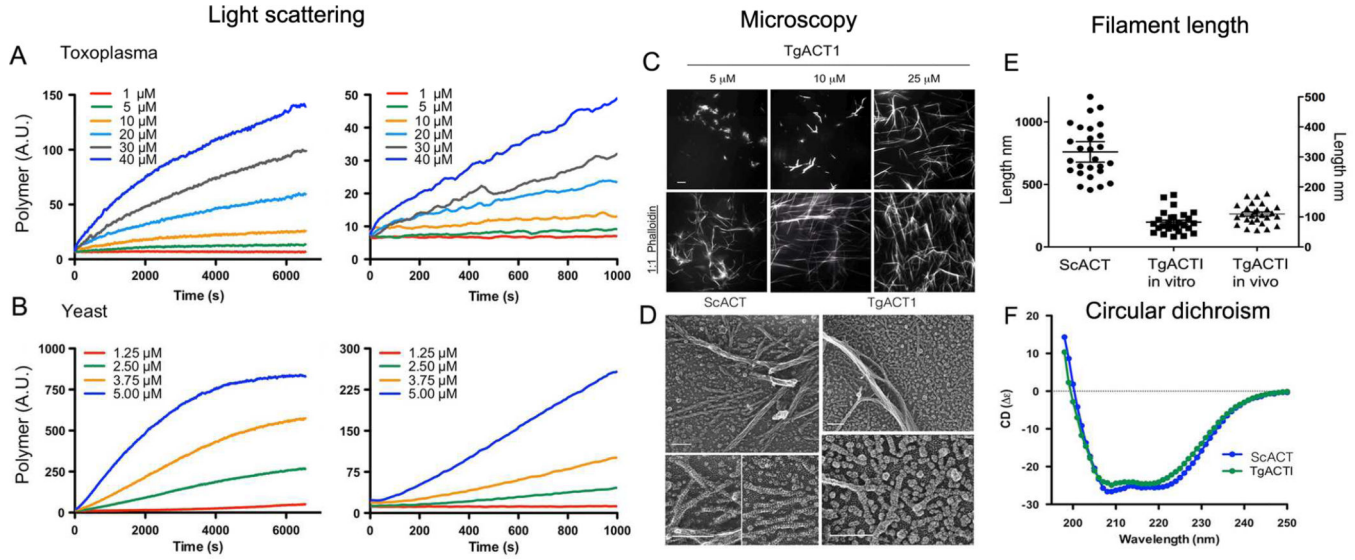

Figure 1. Concentration dependent polymerization of TgACTI vs ScACT

(**A**) Light scattering (arbitrary units, A.U.) vs. concentrations (μM) of TgACTI. Plot at right shows the initial time course expanded to highlight the lack of lag phase. (B) Light scattering (arbitrary units, A.U.) *vs*. concentrations (μM) of ScACT. Initial plots show evidence of lag (expanded plot at right), and plateau at later time points. (**C**) Fluorescence microscopy of polymerized TgACTI visualized with 0.33 μM Alexa 488-phalloidin ± equimolar amounts of unlabeled phalloidin (1:1). Scale bar = 5 μm. (**D**) Quick-freeze, deep-etch electron micrographs of ScACT (5 μM) *vs*. TgACTI (40 μM) polymerized in F buffer. Scale bars = 100 nm. (**E**) Lengths of actin filaments measured *in vitro* for ScACT and TgACTI as in D, or for TgACTI *in vivo* as reported previously[8]. Left y-axis, ScACT, right y-axis, TgACTI. Means ± S.D. (**F**) Circular dichroism measurements of purified ScACT vs. TgACTI, 0.4 μM. All panels are representative experiments of three or more similar experiments.

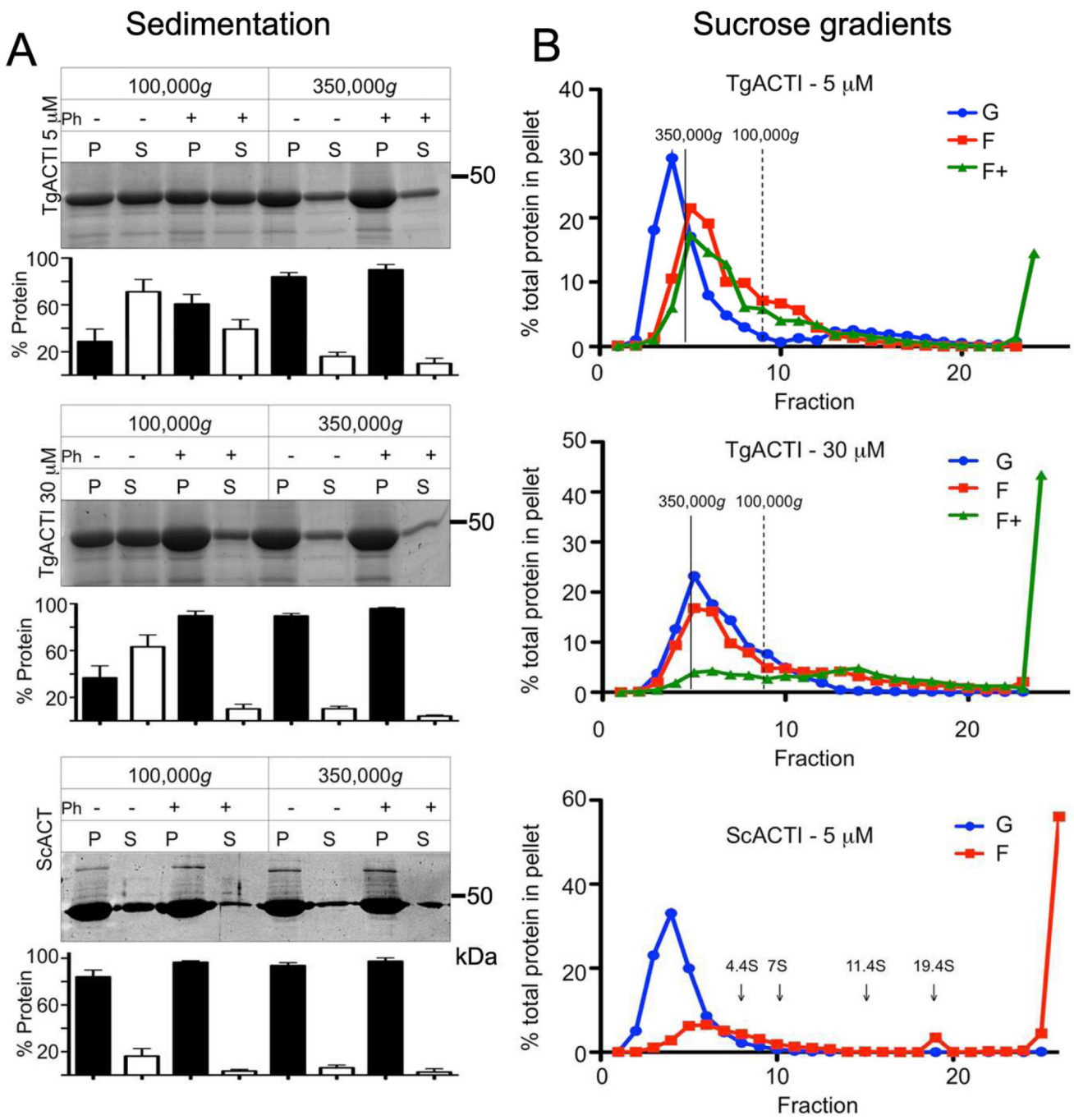

Figure 2. TgACTI forms small heterogeneous polymers

(**A**) TgACTI (5 µM top *vs*. 30 µM middle) was polymerized in F buffer for 1 h at room temperature ± equimolar phalloidin (Ph) and centrifuged at 100,000*g* or 350,000*g* for 1 h at room temperature. Pellet (P) or precipitated supernatant (S) fractions were resolved on a 12% SDS-PAGE gel, stained with SYPRO Ruby, and quantified by phosphorimager analysis. ScACT (5 µM, bottom) was analyzed in parallel. Mean ± S.D., n = 3 or more experiments combined in graphs; representative gels are shown. (**B**) Sedimentation of TgACTI (5 µM top, 30 µM middle) in G buffer (G, blue), F buffer (F, red) or F buffer with

equimolar phalloidin (F+, green) by sucrose density centrifugation. ScACT (5 μM) was analyzed in a parallel gradient. Dashed and solid black lines correspond to the proportion of TgACTI that would be found in the 100,000*g* and 350,000*g* pellets under standard sedimentation conditions as in A. Size standards denoted with black arrows. Representative of 3 or more similar experiments.

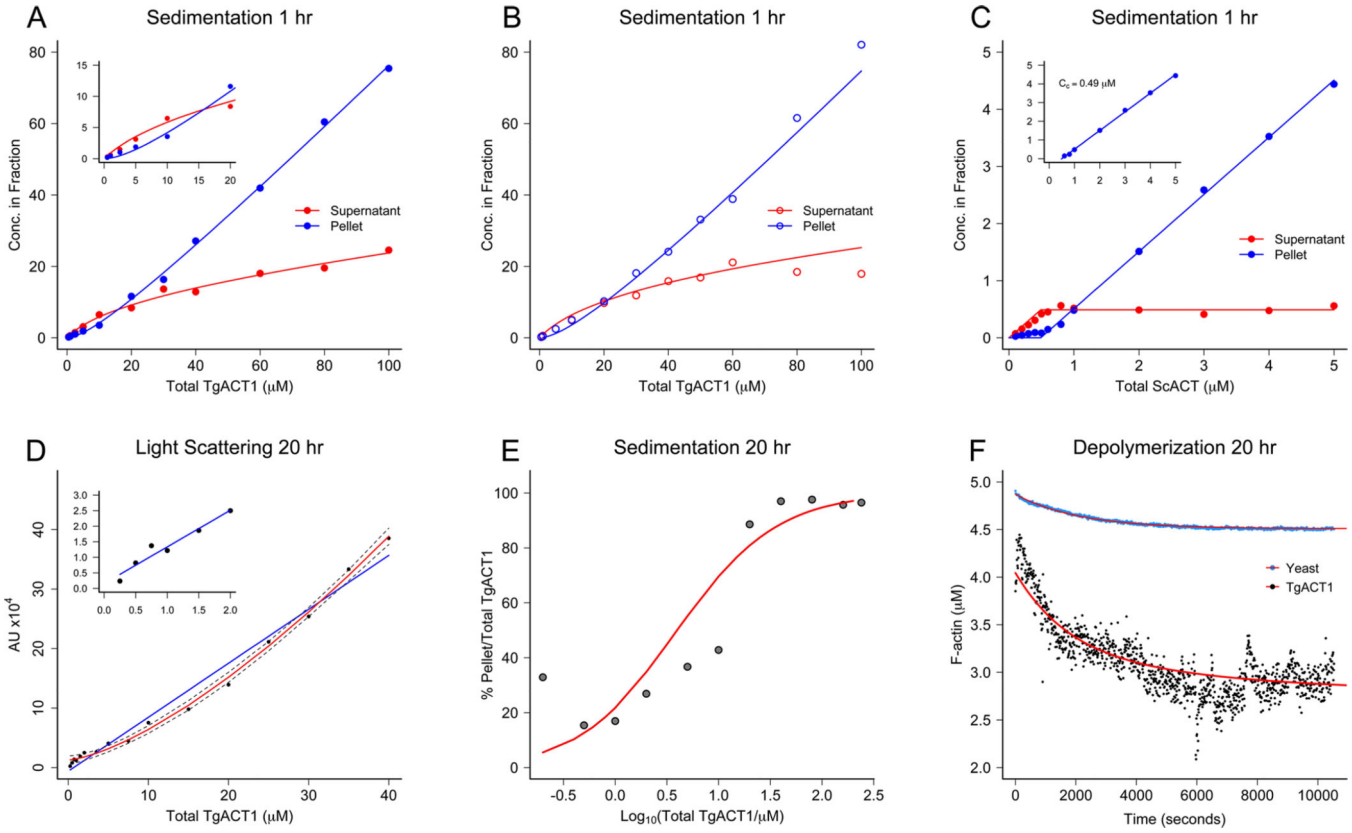

Figure 3. TgACTI polymerizes by an isodesmic process

(**A**) Polymerization of TgACTI in F buffer pH 8.0 for 1 h followed by centrifugation at 100,000*g* for 1 h at room temperature. The points are experimental results for the concentration of protein in the pellet (blue) or supernatant (red), plotted versus initial total concentration. The solid-line curves are the results of simulations using the isodesmic model. Inset shows the concentration range from 0.5 – 20 μM. (**B**) Similar sedimentation analysis performed as in (A) except KMEI (see methods) pH 7.2. (C) Polymerization of yeast actin (ScACT) in F buffer pH 8.0 for 1 h followed by centrifugation at 100,000*g* for 1 h at room temperature. Inset shows linear regression plot of lower concentrations (0.5 – 5 μM) used to estimate the Cc. (D) Polymerization of TgACTI in F-buffer at steady state (i.e. 20 h), as monitored by light scattering. Linear regression (blue) or nonlinear (red) fit curves. Dotted line indicates 95% confidence interval. Mean, n ≥ 3 experiments. Lower concentrations are expanded in inset. (**E**) Sedimentation of TgACTI polymerized to steady state in F buffer for 20 h. Centrifugation at 100,000*g* for 1 h at room temperature. The points are experimental data, and the solid curve is the result of a simulation with the isodesmic model. (**F**) Dilution-induced depolymerization of TgACTI vs. ScACT. Steady-state samples polymerized for 20 h were diluted 4-fold in F buffer, and depolymerization was monitored by light scattering. The red curve is the prediction from the isodesmic model for TgACTI and from a nucleation-elongation model for ScACT. Unless otherwise noted, all panels are representative experiments of three or more similar experiments.

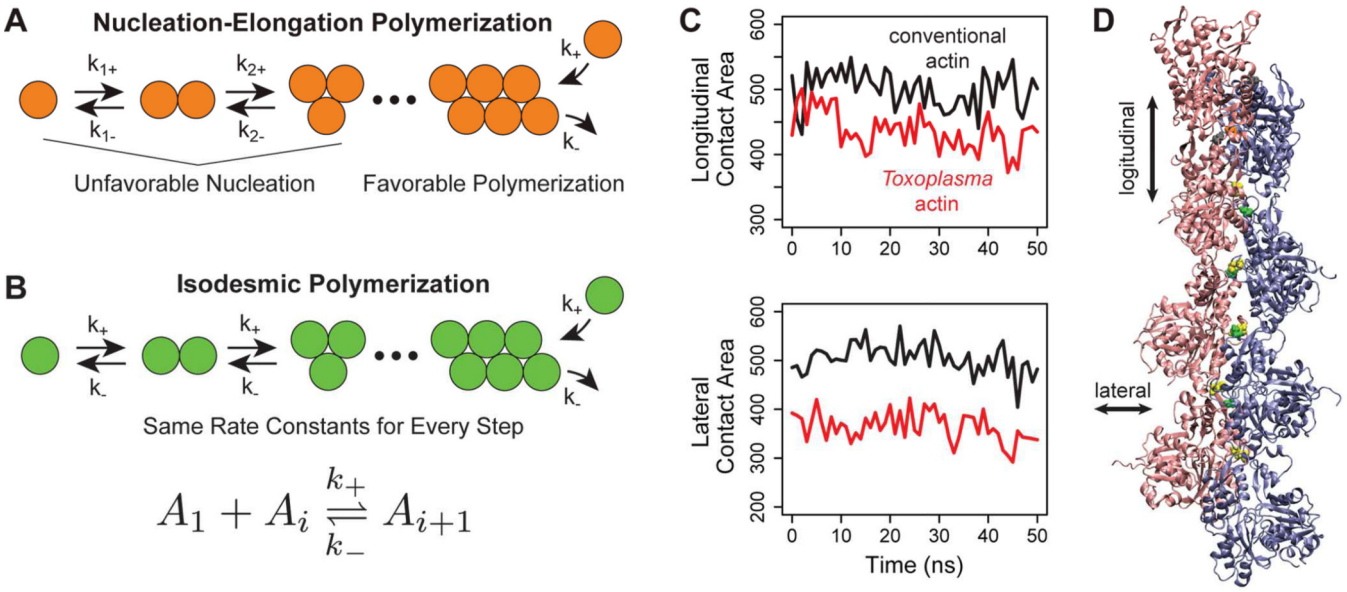

Figure 4. Modeling filament polymerization and dynamics

(**A, B**) Standard nucleation-elongation mechanism *vs*. isodesmic model. Under isodesmic polymerization the on rate (k_+) and off rate (k_-) are the same for every monomer addition, independent of length. (**C**) Molecular dynamics simulation reflects a propensity for weaker lateral interactions in *Toxoplasma vs*. muscle actin filaments (conventional). (**D**) Key amino acid differences that were predicted to alter the lateral interaction between protofilaments[11] are highlighted in yellow and green, while the two strands of the filament are colored blue and pink.

Table 1

Dynamic light scattering of actins in solution

Sample	G Buffer				F buffer			
	Rh (nm)[a]	Molecular weight[b]	PD[c]	Int[d]	Rh (nm)	Molecular weight	PD[c]	Int[d]
TgACTI 1 μM	4.7	128	12	81.6	nd	nd	nd	nd
TgACTI 5 μM	7.2	344	22	89	26.3	7,015	33.0	87
ScACT 1 μM	3.6	67	27	81	3,656	731,106,000	0	92

[a] estimate of hydrodynamic radius = Rh

[b] Estimated from Rh, given in kDa

[c] % Polydispersity

[d] % Intensity of scattered light

nd not determined